J. Phys. C: Solid State Phys. **21** (1988) 4663–4668. Printed in the UK

On the coexistence of ferro- and antiferromagnetic spin fluctuations and their contributions to the specific heat

H Fehske and D Ihle
Sektion Physik, Karl-Marx-Universität, Karl-Marx-Platz, 7010 Leipzig, German Democratic Republic

Received 25 February 1988

Abstract. On the basis of a uniaxially anisotropic quasi-particle band model and the resultant wavevector-dependent response function, the coexistence of ferro- and antiferromagnetic spin fluctuations and their effects on the low-temperature specific heat (mass enhancement, $T^3 \ln T$ law) of exchange-enhanced paramagnetic systems are studied in the framework of paramagnon theory. The results are related to the localised-paramagnon approximation. Our anisotropic spin-fluctuation model may explain the results of both the specific heat and neutron scattering experiments on UPt_3.

The study of Fermi surface (FS) geometry effects on the low-frequency-fluctuation contributions to the low-temperature specific heat C_v (mass enhancement, $T^3 \ln T$ term) in the normal phase of heavy-fermion systems, e.g. of UPt_3, described by Anderson lattice models (Millis 1987, Rasul and Harrington 1987) or paramagnon models (Konno and Moriya 1987, Ihle and Fehske 1988 (hereafter referred to as I)) is of particular interest. Taking as a basis the uniaxially anisotropic quasi-particle band model (Fehske and Ihle 1987)

$$\varepsilon_k = \tfrac{1}{2}(k_x^2 + k_y^2) - \alpha \cos k_z \tag{1}$$

we have investigated in I the effects of FS anisotropy and topology (a closed FS for $-\alpha < \varepsilon_F < \alpha$, an open FS for $\varepsilon_F > \alpha$; ε_F is the Fermi energy) on the spin-fluctuation (SF) contributions to C_v of exchange-enhanced paramagnetic metals, and have found qualitatively novel SF phenomena as compared with the results obtained with isotropic paramagnon models. As revealed by the reduced static susceptibility $\bar{\chi}(\boldsymbol{q}) = \chi_0(\boldsymbol{q})/N_0(\varepsilon_F)$, where (i) $N_0(\varepsilon_F) = \Omega d_\parallel / 4\pi^2$, (ii) $d_\parallel = 2 \cos^{-1}(1-\xi)\theta(2-\xi) + 2\pi\theta(\xi - 2)$, and (iii) $\xi = 1 + \varepsilon_F/\alpha$, in the closed-FS region $1 < \xi < 2$, the SF model describes various types of SF, in particular the coexistence of differently exchange-enhanced ferromagnetic (FM) SF perpendicular to the anisotropy axis and antiferromagnetic (AFM) SF along the anisotropy axis. Both kinds of SF contribute to the mass enhancement and can lead to a linear dependence of the mass enhancement on the Stoner factor. For either FS topology we have obtained the $T^3 \ln T$ law, where its temperature range of validity increases with the FS anisotropy. Furthermore, in I we have developed an anisotropic SF model for UPt_3 which may explain both the C_v

0022-3719/88/264663 + 06 $02.50

(including pressure-dependent data) and neutron scattering experiments (Aeppli *et al* 1987) revealing AFM SF along the hexagonal axis.

In this paper we present a more elaborate study of the coexistence of FM and AFM SF and their contributions to C_v. Our goals are (i) to analyse the contributions of FM and AFM SF to the mass enhancement as functions of the FS anisotropy (determined by ξ) and the Stoner factor, (ii) to include the finite-wavevector properties of $\bar{\chi}_0(\boldsymbol{q})$ in the calculation of the full temperature dependence of C_v and of the $T^3 \ln T$ term, and (iii) to relate our results to the localised-paramagnon picture given by Konno and Moriya (1987). We start from the C_v expression derived in I in the framework of paramagnon theory,

$$C_v = \gamma T + \frac{36}{\pi}\gamma_0 \varepsilon_F \left(\frac{2\pi}{d_\parallel}\right)^4 \frac{\xi^3}{\xi - 1}\left(\frac{T}{\bar{T}_F}\right)^3 J\left(\frac{T}{\bar{T}_F}\right) \tag{2}$$

$$\gamma = \gamma_0(1+\lambda_{SF}) \qquad \lambda_{SF} = \left(\frac{2\pi}{d_\parallel}\right)^2 \frac{(S-1)}{S}\frac{6\pi}{\Omega}\sum_{\boldsymbol{q}} u(\boldsymbol{q})(S(\boldsymbol{q})-1) \tag{3}$$

$$J\left(\frac{T}{\bar{T}_F}\right) = \int_0^\infty \mathrm{d}x\, x^4 n'(x) \frac{2\pi^2}{\Omega}\sum_{\boldsymbol{q}}\left(u(\boldsymbol{q})\frac{S(\boldsymbol{q})}{S}\right)^3 \left[1+\left(\frac{4\pi^2}{d_\parallel}\xi x \frac{T}{\bar{T}_F}u(\boldsymbol{q})\frac{S(\boldsymbol{q})}{S}\right)^2\right]^{-1} \tag{4}$$

$$\bar{T}_F = \varepsilon_F \xi/(S-1)(\xi-1) \qquad S(\boldsymbol{q}) = \{1-[(S-1)/S]\bar{\chi}_0(\boldsymbol{q})\}^{-1} \tag{5}$$

where $S \equiv S(0) = (1 - IN_0(\varepsilon_F))^{-1}$ (I = intra-site quasi-particle interaction) is the Stoner factor, $\gamma_0 = \frac{2}{3}\pi^2 N_0(\varepsilon_F)$, and $n(x) = (\mathrm{e}^x - 1)^{-1}$. The function $u(\boldsymbol{q})$ is obtained from the calculation of $\mathrm{Im}\,\chi_0(\boldsymbol{q}, \omega) = (\Omega/\alpha)\omega u(\boldsymbol{q})$ for $\omega/|\boldsymbol{q}| \ll 1$ and is reasonably well approximated by its expansion for $|\boldsymbol{q}| \ll 1$ given, for the closed FS, by

$$u(\boldsymbol{q}) = \{\pi^2 q_\parallel [2(z_1 - z_2)]^{1/2}\}^{-1} K\left(\frac{(z_1-1)(z_2+1)}{2(z_1-z_2)}\right)^{1/2} \tag{6}$$

$$z_{1,2} = -(q_\perp/q_\parallel)^2 \pm [1 - 2(\xi-1)(q_\perp/q_\parallel)^2 + (q_\perp/q_\parallel)^4]^{1/2}$$

where $q_\perp^2 = (q_x^2 + q_y^2)/\alpha$, $q_\parallel = |q_z|$, and $K(k)$ is the complete elliptic integral of the first kind. Note that $u(\boldsymbol{q})$ has a $|\boldsymbol{q}|^{-1}$ divergence for $|\boldsymbol{q}| \to 0$, and $|\boldsymbol{q}|u(\boldsymbol{q})$ shows a maximum for $q_\perp \simeq q_\parallel$.

Let us first consider $\bar{\chi}_0(\boldsymbol{q}) = \bar{\chi}_0(q_\perp, q_\parallel)$, depicted in figure 1. $\bar{\chi}_0(\boldsymbol{q})$ exhibits a maximum at $\boldsymbol{q} = 0$ for $0 < \xi < 1$ (figure 1(*a*)) or at $\boldsymbol{Q} = (0, 0, \pi)$ for $1 < \xi < 2$ (figures 1(*b*) to 1(*d*)), where near the topological transition ($\xi = 2$) $\bar{\chi}_0(\boldsymbol{q})$ shows a remarkable flattening. In the coexistence region of FM and AFM SF ($1 < \xi < 2$) the properties of $\bar{\chi}_0(\boldsymbol{q})$ lead to the following condition on S (see I):

$$S < S_m \equiv \bar{\chi}_0(0,\pi)(\bar{\chi}_0(0,\pi) - 1)^{-1}. \tag{7}$$

From (3) we calculate the SF-mediated mass enhancement, defined by $1 + \lambda_{SF}$, where we use the full dependence on $\boldsymbol{q}$ of $\bar{\chi}_0(\boldsymbol{q})$ and restrict the integration over $\boldsymbol{q}$ by a cut-off energy (ε_c) surface with the symmetry of the FS, where $\varepsilon_c = q_c^2\xi - 1$ and $q_c = 1.6$ (see I). The results for λ_{SF} as a function of S and ξ are shown in figure 2. Compared with the convex function $\lambda_{SF}(S)$ due to FM SF for $0 < \xi < 1$ (plotted for $\xi = 0.5$), where for large S we have $\lambda_{SF} \propto \ln S$, in the region $1 < \xi < 2$ the behaviour of $\lambda_{SF}(S)$ for $S \leqslant S_m$ is qualitatively changed by the combined effects of all the SF. With increasing ξ, the dependence of λ_{SF} on S varies from a nearly linear increase for all $S < S_m$ (figure 2: $\xi = 1.1$) to a stronger-than-linear increase as S approaches S_m, where near the topological

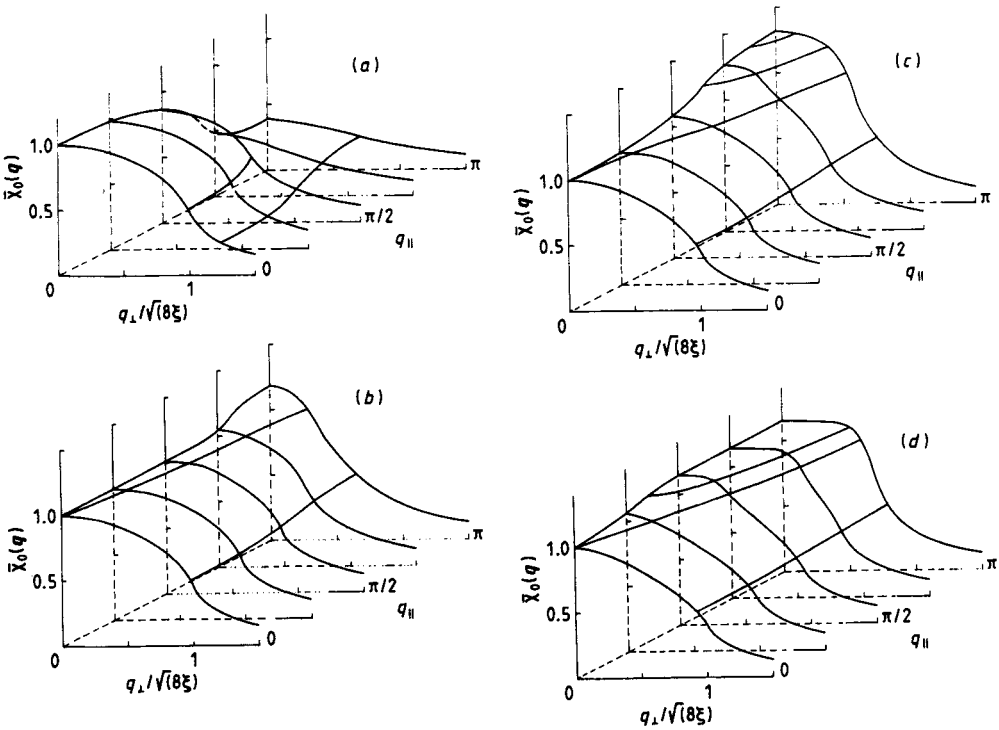

Figure 1. The static susceptibility of the model (1): (*a*) $\xi = 0.5$; (*b*) $\xi = 1.1$; (*c*) $\xi = 1.5$; (*d*) $\xi = 1.9$.

transition ($\xi = 1.9$) the mass enhancement becomes very large. In order to obtain insight into the peculiar dependence on S and ξ of λ_{SF} and to distinguish more precisely between the contributions to λ_{SF} from the various SF, in figure 3 we show the integrand $L(\boldsymbol{q}) \equiv u(\boldsymbol{q})(S(\boldsymbol{q}) - 1)$ in (3) along the anisotropy axis for the ξ-values ($1 < \xi < 2$) belonging to the curves in figure 2. The mass enhancement is mainly determined by SF with wavevectors for which $L(\boldsymbol{q})$ is large. For all ξ we get a remarkable contribution to λ_{SF} from SF with wavevectors around $\boldsymbol{q} = 0$. The contribution from shorter-wavelength and AFM SF is reflected by the enhancement of $L(\boldsymbol{q})$ in a region of finite $\boldsymbol{q}$ up to the Brillouin zone boundary ($q_\parallel = \pi$) and increases considerably with ξ and S. This behaviour is mainly caused by the peculiar dependence on $\boldsymbol{q}$ of $\bar{\chi}_0(\boldsymbol{q})$ (figure 1) and results in the concave functions $\lambda_{SF}(S)$ given in figure 2. Note that in the SF model for UPt_3 suggested in I and referring to the FS region $1 < \xi < 2$, the Wilson ratio $R \equiv (\chi/\chi_0)(\gamma/\gamma_0)^{-1} = S(1 + \lambda_{SF})^{-1}$ (χ = zero-temperature magnetic susceptibility) obtained from figure 2 for different values of ξ and S lies in the range $1 < R < 1.5$, in agreement with experiments.

Now we evaluate the SF contribution (2) to C_v beyond the γT term, i.e. the full temperature dependence, in the region $1 < \xi < 2$. Whereas in I we have used the approximation $S(\boldsymbol{q}) = S$, here we use the full dependence on $\boldsymbol{q}$ of $S(\boldsymbol{q})$. This yields a weaker decrease of $C_v/\gamma_0 T$ with T compared with the result obtained using $S(\boldsymbol{q}) = S$, as shown in figure 4. In order to obtain the low-temperature dependence, in figure 5 we plot $-J$ as a function of $\ln(\bar{T}_F/T)$ for $\xi = 1.1$. For $T < T_m$ we obtain $J = a \ln(T/T_{SF})$, $T_{SF} = b\bar{T}_F$. Figure 5 shows that the coefficient a in the $T^3 \ln T$ term does not depend on

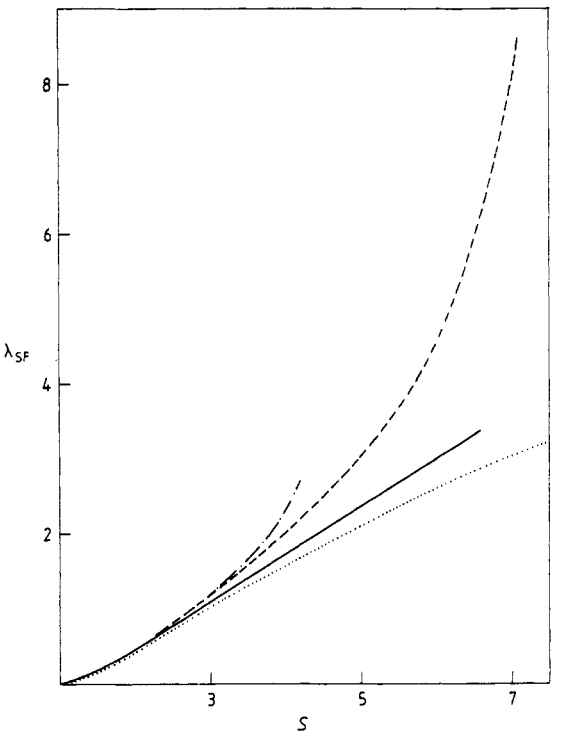

Figure 2. Mass enhancement. Full curve, $\xi = 1.1$; chain curve, $\xi = 1.5$; broken curve, $\xi = 1.9$; dotted curve, $\xi = 0.5$.

the structure of $S(\boldsymbol{q})$. With $S(\boldsymbol{q}) = S$ we have $T_m \simeq \frac{1}{12}\bar{T}_F$ and $b \simeq 0.4$ (see I), so $T_m \simeq 0.2\,T_{SF}$. The inclusion of the dependence on $\boldsymbol{q}$ of $S(\boldsymbol{q})$ results in a decrease of $T_m/\bar{T}_F$ and b with increasing S by a factor smaller than about two, where for $\xi = 1.1$ we get $T_m \simeq 0.14\,T_{SF}$. Comparing the experimental range of validity of the $T^3 \ln T$ law for UPt_3, $T_m^{exp} \simeq 5$–$20\ K$, with T_m in our SF model, we use $T_{SF}^{exp} \simeq 25$–50 K (which has to be equated, by a fitting procedure, to the theoretical expression for T_{SF}) and obtain $T_m \simeq 0.2\,T_{SF} \simeq 5$–$10$ K, in rather good agreement with experiments.

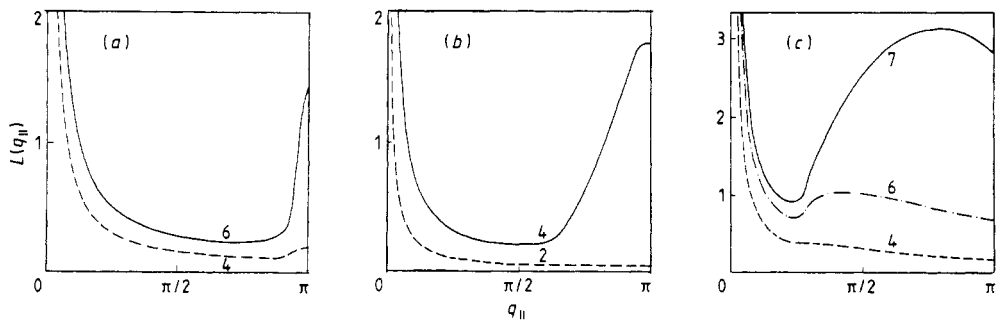

Figure 3. The integrand $L(q_{\parallel})$ in (3): (*a*) $\xi = 1.1$; (*b*) $\xi = 1.5$; (*c*) $\xi = 1.9$. The values on the curves are of S.

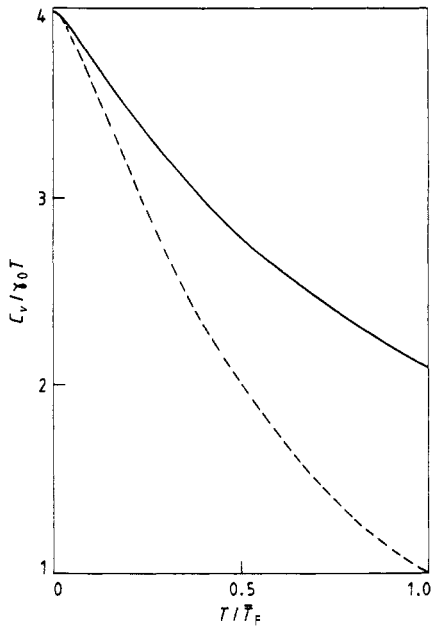

Figure 4. The specific heat $C_v/\gamma_0 T$ for $\xi = 1.1, S = 6$ (full curve), and the approximation $S(q) = S$ (broken curve).

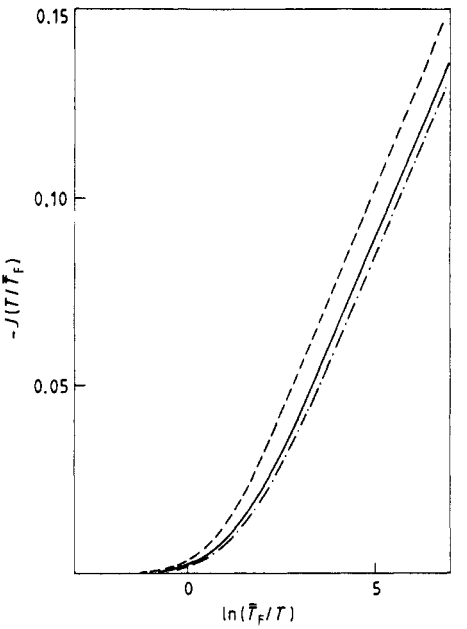

Figure 5. The integral $-J(T/\bar{T}_F)$ (equation (4)) for $\xi = 1.1$. Full curve, $S = 4$; chain curve, $S = 6$; broken curve, the approximation $S(q) = S$.

Recently, Konno and Moriya (1987) have considered the specific heat due to (almost) localised paramagnons characterised by a weakly q-dependent damping Γ_q. Using the approximation $\Gamma_q = \Gamma$, those authors found the $T^3 \ln T$ law to be obeyed in the temperature range $0.7\Gamma/2\pi < T < 3\Gamma/2\pi$ and have attributed the $T^3 \ln T$ term observed for UPt_3 to the localised nature of paramagnons rather than to the contribution from low-q SF components (FMSF). Relating our SF approach to the formulation by Konno and Moriya (1987) (in terms of Γ_q), we have shown that both approaches are identical provided the temperature dependence of the magnetic susceptibility is neglected and Γ_q is replaced by $\Gamma_q = \alpha(I\Omega S(q)u(q))^{-1}$. In particular, putting $\Gamma_q = \Gamma$ in (2), using (4), we get equation (4.1) of Konno and Moriya (1987) yielding the $T^3 \ln T$ law in the temperature range quoted above. In our SF model, including arbitrary-wavevector components of the SF, the dependence on $\boldsymbol{q}$ of Γ_q is governed by $L(\boldsymbol{q}) + u(\boldsymbol{q})$ with $L(q_\parallel)$ plotted in figure 3. We see that Γ_q shows a linear increase in the small-$|\boldsymbol{q}|$ region for all ξ and S, whereas the dependence on $\boldsymbol{q}$ for larger q is strongly affected by the FS anisotropy and Stoner enhancement. For appropriate choices of ξ and S, Γ_q outside the small-$|\boldsymbol{q}|$ region may be well approximated by a mean value, corresponding to the localised paramagnon picture. The divergence of $L(\boldsymbol{q})$ in the limit $|\boldsymbol{q}| \to 0$ removes the lower bound of the temperature interval in which, with $\Gamma_q = \Gamma$, the $T^3 \ln T$-like behaviour is found; i.e., the contribution from SF with $|\boldsymbol{q}| \ll 1$ gives rise to the $T^3 \ln T$ law being valid down to zero temperature, as shown in figure 5. Thus, we conclude that our SF model for UPt_3 incorporating the detailed finite-wavevector properties of the SF (coexistence of FM and AFM SF) may explain the $T^3 \ln T$ law for the specific heat of UPt_3 in the range $0 < T \lesssim 10$ K.

Finally, let us point out that the anisotropy of the FS may result in qualitative effects not only on the structure of SF in paramagnon models but also on the low-frequency quantum fluctuations and their contributions to macroscopic properties in the Anderson lattice models which, however, have not yet been investigated.

References

Aeppli G, Goldman A, Shirane G, Bucher E and Lux-Steiner M-Ch 1987 *Phys. Rev. Lett.* **58** 808
Fehske H and Ihle D 1987 *J. Phys. F: Met. Phys.* **17** 2109
Ihle D and Fehske H 1988 *Phys. Rev.* B at press
Konno R and Moriya T 1987 *J. Phys. Soc. Japan* **56** 3270
Millis A J 1987 *Phys. Rev.* B **36** 5420
Rasul J W and Harrington A P 1987 *J. Phys. C: Solid State Phys.* **20** 4783